DJS Vol. 49(1)(2024) – pp. 79- 89 ISSN: 1012-5965

Delta Journal of Science
Available online at
https://djs.journals.ekb.eg/

Research Article

PHYSICS

Linear modes in the Venusian ionosphere

A.E. Gomaa[1*], N.M. El-Siragy[1], W. M. Moslem[2,3], I. S. Elkamash[4], A.A. El-Bendary[1]

[1] Department of Physics, Faculty of Science, Tanta University, Tanta, P.O. 31527, Egypt.
[2] Department of Physics, Faculty of Science, Port Said University, Port Said 42521, Egypt.
[3] Centre for Theoretical Physics, The British University in Egypt (BUE), El-Shorouk City, Cairo ,Egypt.
[4] Department of Physics, Faculty of Science, Mansoura University, Mansoura 35516, Egypt.

[*]**Corresponding author**: Ahmad Gomaa **Email:** *ahmed_gomaa@science.tanta.edu.eg*

Received: 17/9/2024 **Accepted**: 7/10/2024

KEY WORDS

Venus
ionosphere
linear modes
linear analysis

ABSTRACT

Linear modes were investigated in the plasma environment of the Venusian ionosphere under model approximation. Utilizing data from the Venus Express (VEX) spacecraft, we estimate the physical parameters within the ionosphere at altitudes ranging from 400 to 1000 km. A fluid model is employed, consisting of a collisionless, unmagnetized, homogeneous, isothermal fluid component, which includes Venusian electrons (e) and two types of positive ions, H^+ and O^+. From this model, we derive the linear dispersion relation that governs the behavior of Langmuir mode, H^+, and O^+ ion acoustic modes. Our analysis reveals distinct characteristics of the Langmuir and ion-acoustic modes depending on the temperature and density ratio of the Venusian ionosphere. We notice that the Langmuir mode is not affected by pumping energy. The H^+ and O^+ ion acoustic modes are affected by pumping energy. As altitude increases within the Venusian ionosphere, the frequency of Langmuir mode and H^+ ion acoustic mode increases, but the frequency of O^+ mode decreases. The findings provide insights into the dynamics of the Venusian ionosphere and an understanding of linear modes in extraterrestrial environments that have the same physical behavior.

Introduction

Venus is a terrestrial planet located second from the Sun to Earth. The solar wind interacts directly with the upper atmosphere, forming the ionosphere. A planet's plasma environment, such as the ionosphere, has enough plasma density and temperature to create different plasma waves **(Huba, 1993)**.

The Venusian environment had many wave phenomena and instabilities, such as stable or unstable ion acoustic waves. Understanding these waves, their behavior, and their modes is essential for understanding Venus's climate and its response to solar activity.

Venus attracted a lot of attention in the early days. The Pioneer Venus Orbiter (PVO) and Venus Express (VEX) were the most important spacecraft that continually researched the Venus ionosphere over many years, so they made several ionospheric and atmospheric measurements (**Colin, 1980)**.

VEX successfully flew around Venus's orbit in April 2006, giving a wealth of new data about the Venusian environment from the surface to the highest levels of the ionosphere. VEX has two orbital motions about Venus: dawn-dusk meridian and noon-midnight meridian (**Lundin et al., 2011)**.

These distinct orbits enabled comprehensive mapping of the ionospheric structure and dynamics, revealing critical information about the interactions between solar wind and the planet's atmosphere.

Plasma waves and linear modes are closely related concepts in plasma physics. Plasma waves are collective oscillations of the charged particles in plasma environments. There are two types of them: electromagnetic waves (e.g., Alfvén waves, whistler waves) and electrostatic waves (e.g., Langmuir waves, ion-acoustic waves) **(Stix, 1992)**.

The study of linear modes provides insights on wave propagation, which is important in fields, such as astrophysics and space physics. Linear modes are characterized by small perturbations from equilibrium. The dispersion relation is used to study linear modes. By studying it, we can determine the stability properties **(Mann et al., 1997)**.

Many authors studied the characteristics of waves on Venus for different conditions. For example, **Chettri et al. 2024** studied nonlinear solitary and periodic waves in Venus's upper ionosphere through wave behavior using the Reductive Perturbation Technique (RPT). As discussed by Pioneer Venus Orbiter observations, **Fowler et al. 2024** introduced the magnetic pumping process to Venus, a mechanism that couples the

solar wind to the Venusian ionosphere. **Morsi et al. 2024** studied ion-acoustic structures in the mantle using hydrodynamic description and reductive perturbation theory. They used the Zakharov-Kuznetsov equation and spacecraft measurements to analyze wave packets, explaining electrostatic fluctuations.

Fayad et al., 2021 investigated the propagation properties of weakly nonlinear ion-acoustic waves in the plasma of the Venusian ionosphere. Their plasma model includes two types of positive cold ions and isothermal electrons. Their study finds that the wave phase velocity is supersonic and provides a suitable higher-order correction for describing solitary waves.

The objective of this study is to investigate the linear modes in a plasma environment on the ionosphere of Venus. We used the observed data for the VEX Dawn-Dusk meridian to get estimated values of the physical parameters in the ionospheric region at altitudes from 400 to 1000 km. This paper is organized as follows: section 2 presents model equations, section 3 shows linear analysis and discussion, and section 4 has the conclusion.

Model equations

The fluid model is employed for a collisionless, unmagnetized, Homogeneous, isothermal, and three-fluid system consisting of Venusian electrons (e), two types of Venusian positive ions, namely (H^+ and O^+). The fluid equations for the three-fluid Venusian ionosphere component (j) **(Chen, 1984)** are:

$$\frac{\partial n_j}{\partial t}+\frac{\partial\left(n_j V_j\right)}{\partial x}=0, \qquad (1)$$

$$\frac{\partial V_j}{\partial t}+V_j\frac{\partial V_j}{\partial x}+q_e Q_j\left(\frac{\partial \phi}{\partial x}\right)+\frac{\sigma_j Q_j}{n}\left(\frac{\partial n_j}{\partial x}\right)=0 \qquad (2)$$

Poisson equation that closed the system of Eqs. (1) and (2) is

$$\frac{\partial^2 \phi}{\partial x^2}=\alpha n_e-\gamma n_H-n_O \qquad (3)$$

The charge neutrality condition at equilibrium reads

$$\alpha=\gamma+1 \qquad (4)$$

In Eqs. (1) - (4), $j = H^+, O^+,$ and $e.\ q_e = +$ for H^+ and $O^+,$ and $q_e = -$ for $e.\ n_j$ refers to normalized densities by the unperturbed background density $n_j^{(0)}$, V_j are normalized by oxygen ion acoustic speed $C_s = (k_B T_e/m_O)^{1/2}$. $Q_j = m_O/m_j$ is the relative mass ratio of species j -to- oxygen ions, $\sigma_j = T_j/T_e$ is the temperature ratio of species j -to- electrons. α and γ are the ratios between the unperturbed background e and H^+ densities -to- the unperturbed O^+ density. The time and space variables are normalized by the inverse of the oxygen ion plasma frequency $\omega_{pO}^{-1}=\left(\epsilon_0 m_O/e^2 n_O^{(0)}\right)^{1/2}$ and oxygen ion Debye radius $\lambda_{DO}=\left(k_B T_e \epsilon_0/e^2 n_O^{(0)}\right)^{1/2}$, respectively.

Furthermore, the electrostatic potential ϕ is normalized by the thermal potential $k_B T_e/e$, where k_B is the Boltzmann constant, ϵ_0 is permittivity, and e represents the electron charge.

Linear analysis and discussion

To investigate the linear mode properties, we assume small perturbations around the equilibrium state and consider harmonic oscillations of the form (**Chen, 1984):**

$$\begin{aligned} n_j &= 1 + n_j' \exp i(K - \omega t), \\ V_j &= V_j' \exp i(K - \omega t), \\ \phi &= \phi' \exp i(K - \omega t). \end{aligned} \quad (5)$$

where ω and K are the normalized wave frequency and normalized wavenumber **(Krall et al., 1973)**.

The quantities n_j', V_j', and ϕ' are a small perturbation in the dependent plasma parameters.

Linearizing Eqs. (1) and (2) using Eq. (5) leads to the following perturbed number densities:

$$\begin{aligned} n_e' &= \frac{-K^2 Q_e}{\omega^2 - K^2 Q_e}\phi', \\ n_H' &= \frac{K^2 Q_H}{\omega^2 - \sigma_H K^2 Q_H}\phi', \\ n_O' &= \frac{K^2}{\omega^2 - \sigma_O K^2}\phi'. \end{aligned} \quad (6)$$

After some straightforward algebraic manipulation from Eq. (6) in Eq. (3), we have the linear dispersion relation in the form:

$$1 - \frac{\alpha Q_e}{\omega^2 - K^2 Q_e} - \frac{\gamma Q_H}{\omega^2 - \sigma_H K^2 Q_H} - \frac{1}{\omega^2 - \sigma_O K^2} = 0 \quad (7)$$

To study the behavior of the propagation modes in the Venusian ionosphere, we use the complex frequency $\omega = \omega_r + i\omega_i$ in Eq. (7) and solve it numerically, where ω_r is the real frequency of the wave mode and ω_i is the growth rate. Our numerical analysis reveals that $\omega_i = 0$.

Figure (1) displays the real frequency ω_r versus the wave number K for the modes present in our model of the Venusian ionosphere. The results reveal the existence of three distinct modes, each arranged in pairs $\omega_{r,p} (p = 1,2, \ldots,6)$:

- **Langmuir mode**, $\omega_{r,1}(K)$; this mode is accompanied by a negative mirror mode $\omega_{r,6}(K)$, depicted in Fig. (1).
- **(H^+) ion acoustic mode**, $\omega_{r,2}(K)$, It is paired with a negative mirror mode $\omega_{r,5}(K)$, also shown in Fig. (1).
- **(O^+) ion acoustic mode**, $\omega_{r,3}(K)$; this mode is associated with a negative mirror mode $\omega_{r,4}(K)$, presented in Fig. (1).

The results clearly distinguish between modes of positive frequency (propagating in the forward direction) and their corresponding negative frequency counterparts (propagating in the backward direction).

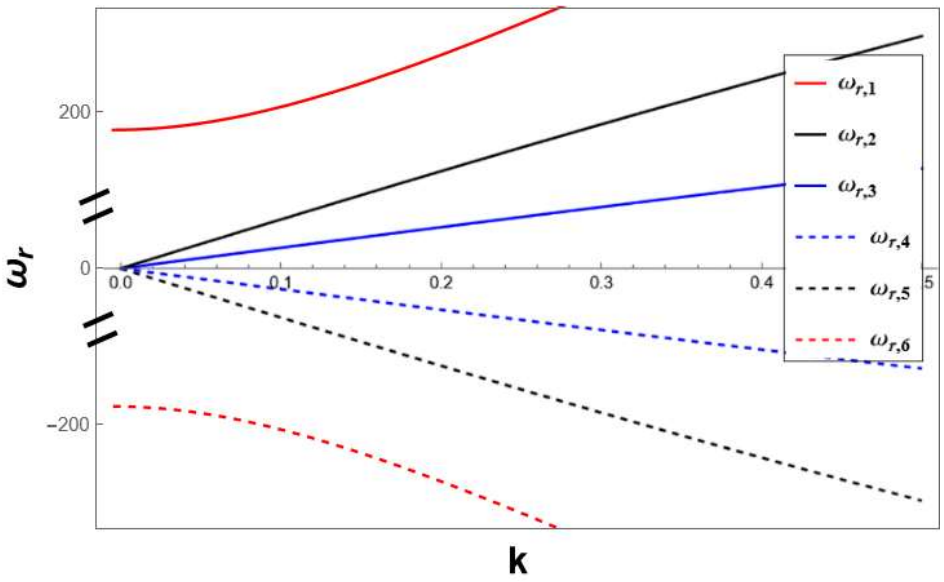

Fig. (1): Real frequency ω_r as a function of wave number K for modes in the Venusian ionosphere. The Langmuir mode $\omega_{r,1}$ is shown in (solid red), accompanied by its negative mirror mode $\omega_{r,6}$ in (dashed red). The (H^+) ion acoustic mode $\omega_{r,2}$ is depicted in (solid black), with its negative mirror mode $\omega_{r,5}$ in (dashed black). The (O^+) ion acoustic mode $\omega_{r,3}$ is presented in (solid blue), paired with its negative mirror mode $\omega_{r,4}$ in (dashed blue). The plasma parameters are $\sigma_O = \sigma_H = 0.1$, $Q_e = 29194.5$, $Q_H = 16$, $\alpha = 1.072$, and $\gamma = 0.072$ **(Lundin et al., 2011; Fayad et al., 2021).**

As shown in Fig. (1), the range of real frequency ω_r of Langmuir mode is higher than H^+ and O^+ ion acoustic modes. Langmuir mode has higher energies than H^+ and O^+ ion acoustic modes.

Fig. (2) shows the relation between the real frequency $\omega_{r,1}$ and the wave number K for the Langmuir mode as a function of temperature ratio σ_H and σ_O. The figure demonstrates that the Langmuir mode has no change with σ_H and σ_O variation. Langmuir mode remains unaffected by energy input into the system, as the characteristic timescale of the Langmuir mode is significantly faster than the timescale associated with ion moving **(Nicholson, 1983).**

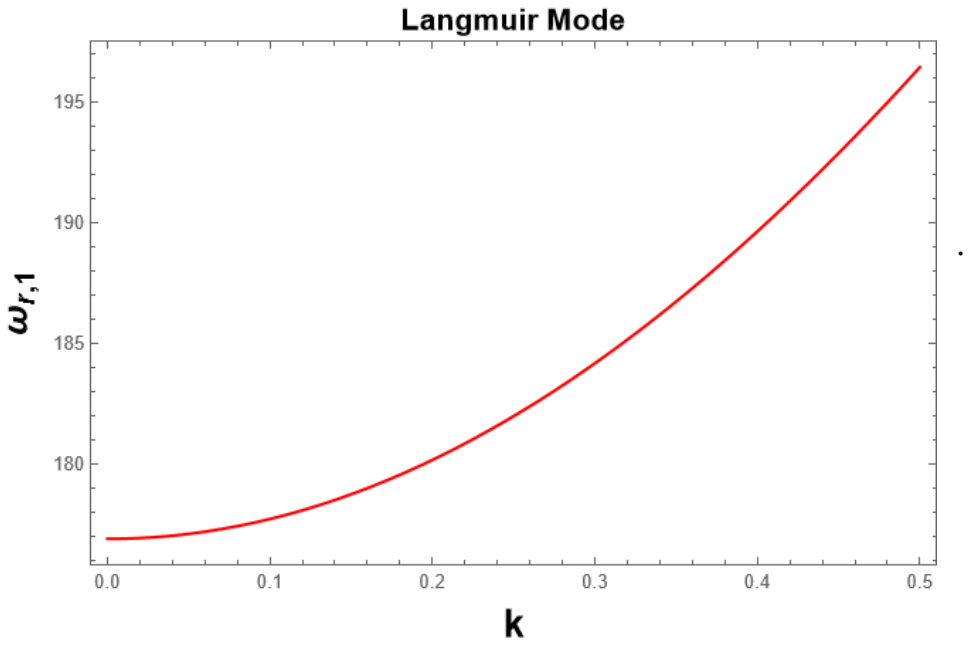

Fig. (2): Real frequency $\omega_{r,1}$ as a function of wave number K for Langmuir mode. The plasma parameters of Q_e, Q_H, α, and γ as of Fig. (1). The solid red line represents cases $\sigma_O = \sigma_H = 0.1$ and 0.2 are coincidences.

Fig. (3) illustrates the relation between the real frequency $\omega_{r,1}$ and the wave number K for the Langmuir mode as a function of varying γ at different altitudes. It is clear from the figure that as γ increases from 0.072 to 0.82. The frequency $\omega_{r,1}$ also increases. An increase in γ is influenced by the corresponding increase in α, $\alpha = 1 + \gamma = \frac{n_e^{(0)}}{n_O^{(0)}}$; increasing in α leads to an increase in the electron number density $n_e^{(0)}$, which makes the Langmuir mode move towards high frequency as described by the electron plasma frequency,

$$\omega_{pe} = \sqrt{\frac{n_e e^2}{\varepsilon_0 m_e}}$$ **(Chen, 1984).**

Fig. (4) illustrates the relation between the real frequency $\omega_{r,2}$ and the wave number K for the hydrogen ion acoustic mode as σ_H with and σ_O. Notably, an increase in $\sigma_H = \sigma_O$ from 0.1 to 0.2 leads to a corresponding increase in the real frequency $\omega_{r,2}$ for specific wave number K. An increase in σ_H and σ_O, (H^+) ion acoustic mode has higher thermal velocity, leading to a higher frequency for (H^+) ion acoustic mode **(Nicholson, 1983)**.

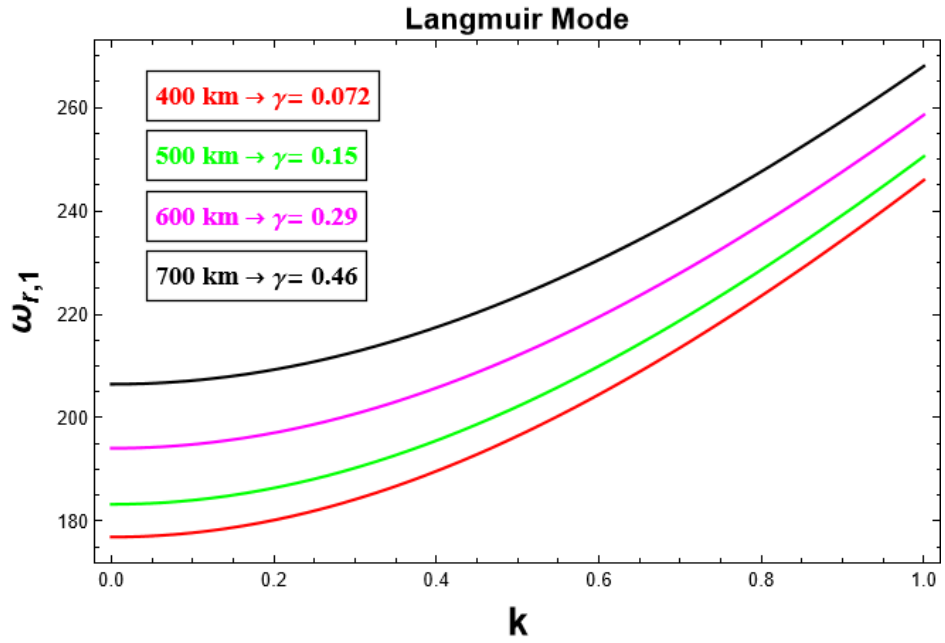

Fig. (3): Real frequency $\omega_{r,1}$ versus wave number K for the Langmuir mode at varying altitudes from 400 km to 700 km. The plasma parameters of σ_H, σ_O, Q_e, and Q_H as of Fig. (1), with $\alpha = 1 + \gamma$.

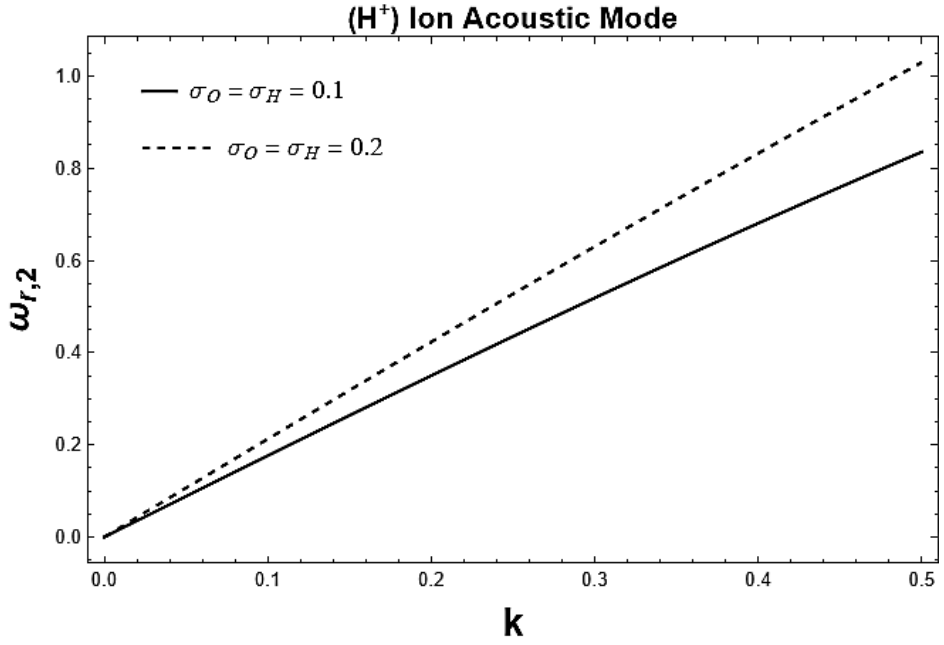

Fig. (4): Real frequency $\omega_{r,2}$ as a function of wave number K for the (H^+) ion acoustic mode. The plasma parameters of Q_e, Q_H, α, and γ as of Fig. (1). $\sigma_O = \sigma_H = 0.1$ (solid black line), $\sigma_O = \sigma_H = 0.2$ (dashed black line).

Figure (5) illustrates the relation between the real frequency $\omega_{r,2}$ and the wave number K for the H^+ ion acoustic mode at altitudes from 400 km to 1000 km. As altitude increases, the ratio $\gamma = n_H^{(0)}/n_O^{(0)}$ also increases. An increase in (H^+) ion acoustic mode density $n_H^{(0)}$, a decrease in the Debye length of (H^+) ion acoustic mode, $\lambda_{DH} = \sqrt{\frac{\varepsilon_0 k_B T}{n_H e^2}}$, which increases (H^+) ion acoustic mode's frequency **(Chen, 1984).**

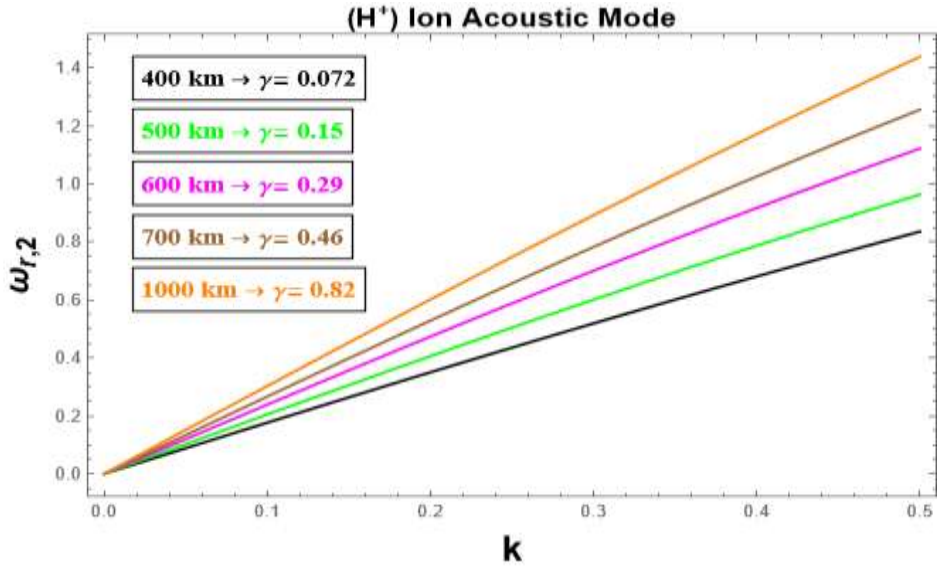

Fig. (5): Real frequency $\omega_{r,2}$ versus wave number K for the (H^+) ion acoustic mode at varying altitudes from 400 km to 1000 km. The plasma parameters of Q_e, Q_H, σ_H, and σ_O as of Fig. (1), with $\alpha = 1 + \gamma$.

Fig. (6) shows the relation between the real frequency $\omega_{r,3}$ and the wave number K for the (O^+) ion acoustic mode, with variations in $\sigma_H = \sigma_O$ from 0.1 to 0.2. The figure illustrates that as σ_H and σ_O increase from 0.1 to 0.2, there is a corresponding increase in the real frequency ω_r for specific wave number K. Physically, an increase in σ_H and σ_O leads to high thermal velocity, a fast decrease in (O^+) ion acoustic mode density $n_O^{(0)}$, an increase in the Debye length of (O^+) ion acoustic mode, time scale of moving and increasing frequency to (O^+) ion acoustic mode **(Nicholson, 1983).**

Finally, Fig. (7) shows the relation between the real frequency $\omega_{r,3}$ and the wave number K for the O^+ ion acoustic mode at altitudes ranging from 400 km to 1000 km. As altitude increases, ratio $\gamma = n_H^{(0)}/n_O^{(0)}$ also increases. An

$\lambda_{DO} = \sqrt{\frac{\varepsilon_0 k_B T}{n_O e^2}}$, and decreases in (O^+) ion acoustic mode's frequency **(Chen, 1984).**

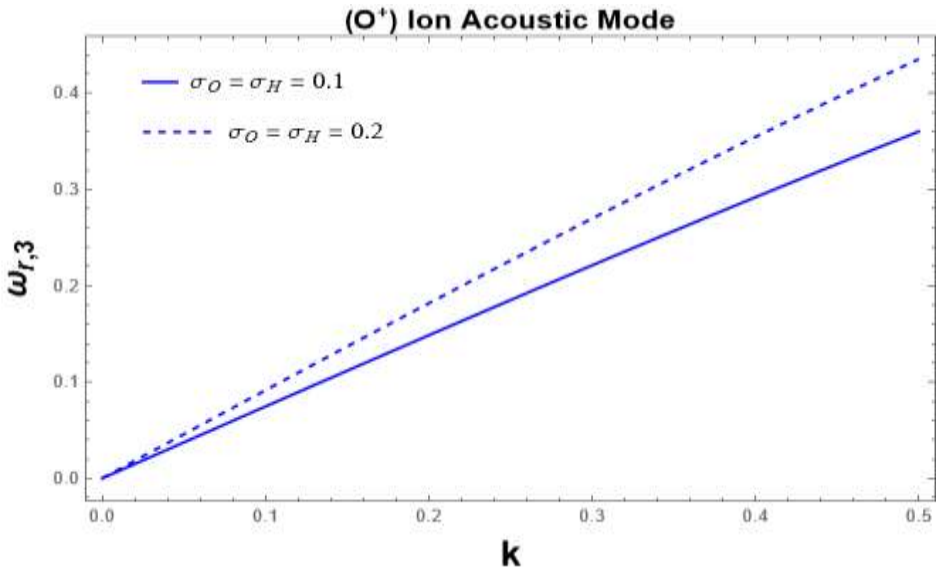

Fig. (6): Real frequency $\omega_{r,3}$ as a function of wave number K for the (O^+) ion acoustic mode. The plasma parameters of Q_e, Q_H, α, and γ as of Fig. (1). $\sigma_O = \sigma_H = 0.1$ (solid blue line), $\sigma_O = \sigma_H = 0.2$ (dashed blue line).

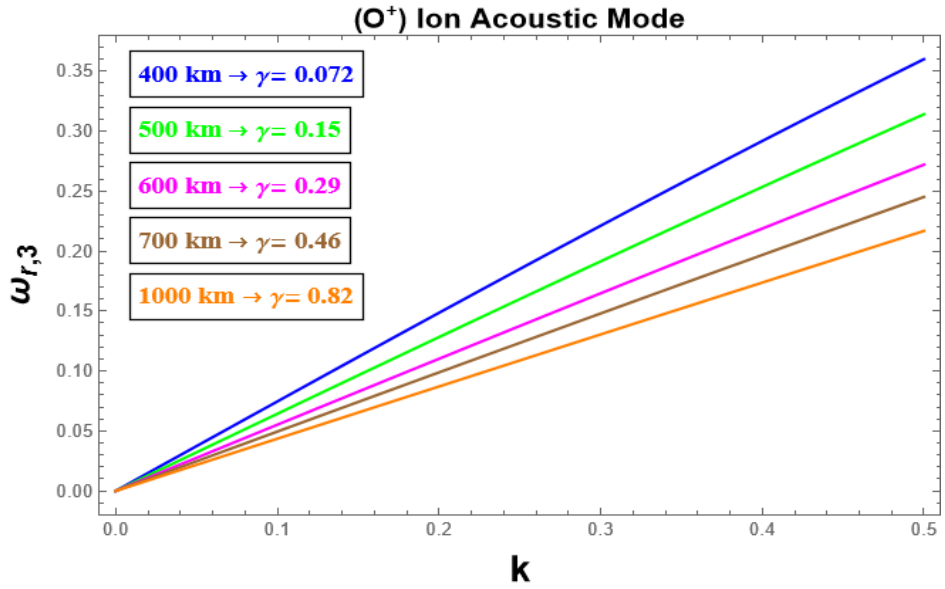

Fig. (7): Real frequency $\omega_{r,3}$ versus wave number K for the (O^+) ion acoustic mode at varying altitudes from 400 km to 1000 km. The plasma parameters of Q_e, Q_H, σ_H, and σ_O as of Fig. (1), with $\alpha = 1 + \gamma$.

Conclusion

We have examined different linear modes within the Venusian ionosphere by utilizing a fluid model of electrons e and two types of ions, H^+ and O^+. By employing observed data from the VEX Dawn-Dusk meridian, we estimated physical parameters relevant to the ionospheric region at altitudes between

400 and 1000 km. Our conclusions can be summarized as follows:

1. H^+ and O^+ ion acoustic modes, and the Langmuir mode exhibit significant variations depending on physical parameters, such as density and temperature ratios.

2. As pumping energy increases within the ionosphere of Venus, the real frequency of both H^+ and O^+ ion acoustic modes increase for a specific value of K. The frequency of Langmuir mode is unaffected by the pumped energy.

3. Based on the model's approximations, as we go up through the Venusian ionosphere (variation in density ratio), the frequency, ω_r of both the Langmuir mode and the H^+ ion acoustic mode increases. The frequency of the O^+ ion acoustic mode decreases.

Future work could study the role of the Venus ionosphere streaming component in the stability of linear modes in the Venusian ionosphere.

References

Chen, (1984): Introduction to plasma physics and controlled fusion. *Springer*, 1

Chettri K.; Prasad P.; Chatterjee P.; Saha A., (2024): Dynamics of nonlinear ion-acoustic waves in Venus' upper ionosphere. *Adv. Space Res.*, 74(8): 3483-4236.

Colin L., (1980): The pioneer Venus program. *J. Geophy. Res.*, 85(A13):7575–7598.

Fayad A.; Moslem W.; El-Labany S., (2021): Effect of streaming velocity, magnetic field, and higher-order correction on the nature of ion acoustic solitons in the Venusian ionosphere. *Phy. Scripta*, 96(4).

Fowler C.; Frost A.; Agapitov O.; Frahm R.; Xu S., (2024): The transfer of solar wind energy to the Venusian ionosphere through magnetic pumping: Evidence from pioneer Venus orbiter observations. *Geophy. Res. Lett.*, 51(12).

Huba D., (1993): Generation of waves in the Venus mantle by the ion acoustic beam instability. *Geophy. Res. Lett.*, 20(17):1751–1754.

Krall N.; Trivelpiece A.; Gross R., (1973): Principles of Plasma Physics. American *J. Phys.*, 41(12):1380–1381.

Lundin R.; Barabash S.; Futaana Y.; Sauvaud J-A; Fedorov A.; Tejada H., (2011): Ion flow and momentum transfer in the Venus plasma environment. *Icarus*, 215(2):751–758.

Mann; Gottfried; Hackenberg P.; Marsch E., (1997): Linear mode analysis in multi-ion plasmas. *J. Plasma Phys.*, 58(2): 205-221.

Morsi S.; Fayad A.; Tolba R.; Fichtner H.; Lazar M.; Moslem W., (2024): Propagation of nonlinear ion-acoustic fluctuations in the mantle of Venus. *Astronomy & Astrophysics*, 685(A17).

Nicholson D.; Nicholson D., (1983): Introduction to plasma theory, 1.

Stix T., (1992): Waves in plasmas. *Springer Science & Business Media*.

الأوضاع الخطية في بيئة البلازما لطبقة الأيونوسفير في كوكب الزهرة

أحمد جمعه [1]، أ.د. نبيل محمد السراجي[١] ، أ.د. وليد مسلم مسلم[٢،٣] ، د. إبراهيم القماش[٤] ، أ.م.د. عاطف أحمد البنداري[١]

[١] قسم الفيزياء، كلية العلوم، جامعة طنطا، طنطا، ص.ب. ٣١٥٢٧، مصر .

[٢] قسم الفيزياء، كلية العلوم، جامعة بورسعيد، بورسعيد ٤٢٥٢١، مصر .

[٣] مركز الفيزياء النظرية، الجامعة البريطانية في مصر(BUE) ، مدينة الشروق، القاهرة، مصر .

[٤] قسم الفيزياء، كلية العلوم، جامعة المنصورة، المنصورة ٣٥٥١٦، مصر.

قمنا بدراسة الأوضاع الخطية في طبقة الأيونوسفير لكوكب الزهرة. استندت دراستنا إلى بيانات مركبة فينوس إكسبريس (VEX) لتقدير الخصائص والقيم الفيزيائية في الأيونوسفير على ارتفاعات تتراوح بين ٤٠٠ و١٠٠٠ كم. قمنا باستخدام نموذج ال (fluid model) الذي يتكون من مكونات متجانسة وغير مغناطيسية و غير متصادمه ، يشمل الإلكترونات (e) ونوعين من الأيونات الموجبة، وهما H^+ و O^+. من خلال هذا النموذج، استنتجنا علاقة التشتت التي تحدد سلوك وضع لانغمور (Langmuir) وكذلك الأيونات الصوتية H^+ و O^+. أظهرت نتائجنا خصائص مميزة لأوضاع لانغمور والأيونات الصوتية، والتي تتأثر بالحرارة والكثافة في الغلاف الأيوني لكوكب الزهرة. لاحظنا أن وضع لانغمور لا يتأثر بالطاقة المضخة، بينما تتأثر أوضاع الأيونات الصوتية H^+ و O^+ بهذه الطاقة. مع زيادة الارتفاع في الأيونوسفير، تزداد ترددات وضع لانغمور ووضع الأيون الصوتي H^+ ، بينما تقل ترددات وضع O^+.